

- our symmetric, nonlinear  $I-V_{xx}$  traces in terms of a simple Joule heating model is unlikely. Second, critical fluctuations are generally expected to lead to universal nonlinearities in the response. See, for example, N. Goldenfeld, *Lectures on Phase Transitions and the Renormalization Group* (Addison-Wesley, Reading, MA, 1992).
7. D. H. Lee and M. P. A. Fisher, *Phys. Rev. Lett.* **63**, 903 (1989).
  8. M. P. A. Fisher, *ibid.* **65**, 923 (1990); C. A. Lütken and G. G. Ross, *Phys. Rev. B* **48**, 2500 (1993).
  9. J. K. Jain, *Phys. Rev. Lett.* **63**, 199 (1989).

10. E. Shimshoni, S. L. Sondhi, D. Shahar, in preparation.
11. A. M. Dykhne and I. M. Ruzin, *Phys. Rev. B* **50**, 2369 (1994); I. M. Ruzin and S. Feng, *Phys. Rev. Lett.* **74**, 154 (1995).
12. D. Shahar *et al.*, in preparation.
13. We thank L. W. Engel, M. P. A. Fisher, S. M. Girvin, S. A. Kivelson, and M. Stone for instructive discussions. Supported by the National Science Foundation and the Beckman Foundation.

13 June 1996; accepted 3 September 1996

## Seismic Evidence for a Low-Velocity Zone in the Upper Crust Beneath Mount Vesuvius

A. Zollo, P. Gasparini, J. Virieux, H. le Meur, G. de Natale, G. Biella, E. Boschi, P. Capuano, R. de Franco, P. dell'Aversana, R. de Matteis, I. Guerra, G. Iannaccone, L. Mirabile, G. Vilardo

A two-dimensional active seismic experiment was performed on Mount Vesuvius: Explosive charges were set off at three sites, and the seismic signal along a dense line of 82 seismometers was recorded. A high-velocity basement, formed by Mesozoic carbonates, was identified 2 to 3 kilometers beneath the volcano. A slower ( $P$ -wave velocity  $V_p \approx 3.4$  to 3.8 kilometers per second) and shallower high-velocity zone underlies the central part of the volcano. Large-amplitude late arrivals with a dominant horizontal wave motion and low-frequency content were identified as a  $P$  to  $S$  phase converted at a depth of about 10 kilometers at the top of a low-velocity zone ( $V_p < 3$  kilometers per second), which might represent a melting zone.

In 1994 a seismic tomography study of the structure and magmatic system beneath Mount Vesuvius was initiated. A two-dimensional (2D) seismic experiment was implemented to determine the feasibility of a three-dimensional (3D) tomography of the volcano, which is located in a densely populated and noisy area.

Mount Vesuvius is a strato-volcano consisting of a volcanic cone (Gran Cono) that was built within a summit caldera (Mount Somma). The Somma-Vesuvius complex has formed over the last 25,000 years by means of a sequence of eruptions of variable explosiveness, ranging from the quiet lava outpourings that characterized much of the

latest activity (for example, from 1881 to 1899 and from 1926 to 1930) to the explosive Plinian eruptions, including the one that destroyed Pompeii and killed thousands of people in 79 A.D. At least seven Plinian eruptions have been identified in the eruptive history of Somma-Vesuvius (1). Each was preceded by a long period of quiescence, which in the case of the 79 A.D. eruption lasted about 700 years. These eruptions were fed by viscous water-rich phonolitic to tephritic phonolitic magmas that appear to have differentiated in shallow crustal conditions. They are believed to have gradually filled a reservoir where differentiation was driven by compositional convection. A minimum depth of about 3 km was inferred for the top of the magmatic reservoir from mineral equilibria of metamorphic carbonate ejecta (2). Fluid inclusions ( $\text{CO}_2$  and  $\text{H}_2\text{O-CO}_2$ ) in clinopyroxenes from cumulate and nodules indicate a trapping pressure of 1.0 to 2.5 kbar at about  $1200^\circ\text{C}$ , suggesting that these minerals crystallized at depths of 4 to 10 km (3). The differentiated magma fraction was about 30% of the total magma in the reservoir, and a volume of about 2 to 3  $\text{km}^3$  was inferred for the reservoir (4). The magma ascent to the surface occurred through a conduit of possibly 70 to 100 m in diameter (5). A thermal model predicts that such a

reservoir should contain a core of partially molten magma (6) that can be detected by high-resolution seismic tomography.

The most recent activity at Mount Vesuvius (1631 to 1944) was fed by tephritic phonolitic magma filling the conduit. There is no evidence of long residence times of magma in a crustal reservoir at depths greater than 1 km. Eruptive episodes appear to have been triggered by the arrival of new batches of isotopically distinct magma from greater depths that mixed with the magma in the conduit (7). Hence, the petrological evidence indicates a complicated feeding system for Mount Vesuvius in spite of the fact that most of the eruptions occur at the summit and only occasionally occur from lateral vents, which are mostly located along the southern slope of the mountain.

Little is known about shallow crustal structure beneath the volcano. A seismic reflection survey carried out in 1973 in the Bay of Naples identified a west-northwest deepening strong reflector that was interpreted as the top of the Mesozoic carbonate platform underlying the volcano (8). Deep drilling carried out for geothermal purposes on the southern slope of the volcano (Trecase well) reached the Mesozoic carbonate basement at a depth of about 1.885 km [1.665 km below sea level (bsl)] (9). Bouguer gravity anomalies were calibrated with these data and were used to model the deepening of the basement down to about 2.3 km bsl underneath the western edge of the volcano (10). The  $P$  waves reflected by the Mohorovičić discontinuity (Moho) (PmP waves) detected by a Deep Seismic Soundings experiment in the Bay of Naples suggest that the crust under Mount Vesuvius is about 35 km thick (11).

We recorded a 30-km-long north-west-trending seismic profile passing through the center of Mount Vesuvius (Fig. 1). Seismic energy was generated by blasting 340 to 410 kg of explosive at sites S1, S2, and S3, and the signals were recorded at 82 receivers deployed along the profile (12). The shot data from S2 and S3 were combined with

A. Zollo, P. Gasparini, P. dell'Aversana, G. Iannaccone, Dipartimento di Geofisica e Vulcanologia, Università di Napoli "Federico II," Largo S. Marcellino 10, 80138, Napoli, Italy.

J. Virieux, Institut de Geodynamique, CNRS Sophia-Antipolis, France.

H. le Meur and R. de Matteis, Dipartimento di Geofisica e Vulcanologia, Università di Napoli "Federico II," Largo S. Marcellino 10, 80138, and Osservatorio Vesuviano, Napoli, Italy.

G. de Natale, P. Capuano, G. Vilardo, Osservatorio Vesuviano, Napoli, Italy.

G. Biella and R. de Franco, Istituto per le Ricerche sul Rischio Sismico, Consiglio Nazionale delle Ricerche (CNR), Milano, Italy.

E. Boschi, Istituto Nazionale di Geofisica, Roma, Italy.

I. Guerra, Dipartimento di Scienze della Terra, Università della Calabria, Cosenza, Italy.

L. Mirabile, Istituto di Oceanologia, Istituto Universitario Navale, Napoli, Italy.

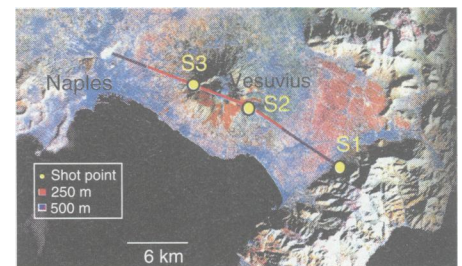


Fig. 1. Satellite image of the Vesuvius area. The shot points and the recording profile for the 1994 active seismic experiment are indicated. Colored segments of the profile are related to different receiver spacing (red = 250 m; blue = 500 m).

40 relocated local earthquakes (13) to provide 176 *P*-wave travel times for the tomographic inversion (14).

The inversion showed a high-velocity region beneath Mount Vesuvius (Fig. 2). Resolution tests showed that although its *P*-wave velocity is poorly resolved by arrival time data from S2, S3, and microearthquakes, it has to be higher than 5 km/s. The region's depth and possible velocity are consistent with those expected for the top of carbonate basement.

A slightly slower ( $V_p \approx 3.4$  to 3.8 km/s) and shallower high-velocity zone extends laterally from Gran Cono to the northern rim of the Somma caldera. The transition to high velocities starts about 400 m below the crater, and the body extends down to at least 3000 m. A shallow 300- to 500-m-thick low-velocity layer ( $V_p < 2.6$  km/s) covers the edifice. It has a greater thickness on the southeast slope where there are more lateral vents. These low velocities are consistent with highly fractured, low-density materials forming the surficial volcanic deposits. Southeast of Gran Cono, velocities are uniformly low (<3 km/s) down to about 2 km bsl.

The 2D ray tracing (15) of early reflected arrivals from shots S2 and S3 indicates the presence of a strong reflector with irregular topography (Fig. 2). Southeast of shot S2, the depth of this reflector correlates with the top of the Mesozoic carbonates, as detected from the Trecase well and gravity data. On the other hand, the top of this reflector matches fairly well the shape of the shallow (from 1.0 to ~3 km of depth), high-velocity (3.5 to 4.0 km/s) region, identified by tomography, beneath Somma-Vesuvius (Fig. 2A). The location, shape, and *P*-wave velocities of this body indicate that it should have a magmatic origin, being either a high concentration of slowly cooled magmatic dikes or a part of the volcano that has suffered an intensive alteration by high-temperature hydrothermal fluids.

Our data do not provide any evidence for a molten magmatic body of more than 0.5 km in diameter down to 4 km of depth. This finding is consistent with the low temperatures (50°C) measured in the Trecase well at a depth of about 2 km (16).

The modeling of arrival times and wave forms from late phases requires the knowledge of a wave velocity function at depths greater than those investigated by the *P*-wave travel-time tomography. The velocity contrast between the layer formed by volcanics and sediments and the underlying carbonates was constrained by modeling of *P*-wave arrivals for shot S1, as detected on vertical seismograms for distances <25 km from the source. This interface (V-L) was assumed to have the shape inferred from the

gravity (10) and Trecase well data. A sharp increase of *P*-wave velocities (from 3.5 to 4.0 km/s up to 5.5 to 6.0 km/s) at the V-L discontinuity was obtained. The depth of the V-L discontinuity and the related *P*-wave velocity contrast are consistent with results from the previous reflection survey (8).

The most peculiar feature observed in the records of S1 at stations at a distance of 10 to 30 km is a prominent wave-amplitude increase at about 8 s (4 to 5 s in reduced times) (Fig. 3A). These large-amplitude late arrivals (LALAs) were detected on the horizontal records rotated along the profile direction and filtered in the 1- to 8-Hz frequency band. The dominant horizontal motion and the low-frequency content of LALAs suggest that this phase is a wave converted from *P* to *S* at a deep discontinuity in the upper crust beneath Vesuvius. A depth of about 10 km was estimated for this discontinuity by a 2D ray-tracing model (17).

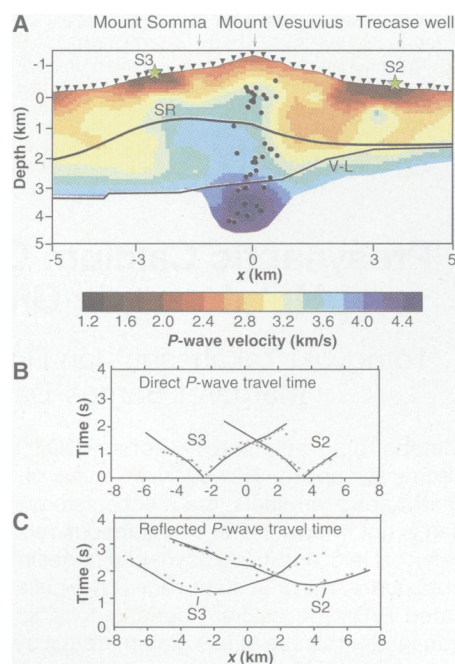


**Fig. 2.** Results of the delay-time tomography and modeling of early reflected phases. **(A)** Inferred 2D model of Vesuvius obtained by tomographic inversion of first *P*-wave arrival times from shots S2, S3, and microearthquakes. Solid circles indicate microearthquake locations. The thick solid line represents the topography of the interface, which is estimated from the arrival times of early reflected waves (shallow reflector, SR). The thin solid line represents the top of the carbonate basement, as inferred from gravity and Trecase well data. **(B)** Misfit between observed (S2, diamonds; S3, circles) and computed (lines) *P*-wave arrival times from shots S2 and S3. **(C)** Misfit between observed (S2, diamonds; S3, circles) and computed (lines) arrival times of the early reflected wave from shots S2 and S3.

We made an independent check of arrival times and amplitudes of this secondary wave forms. These were calculated by a 2D finite difference (FD) code, which computes the complete *P*-*S*<sub>vertical</sub> wave field generated by isotropic seismic sources embedded in a 2D structure (18). A depth of 10 km bsl for the discontinuity that is supposed to produce the *P*-to-*S* conversion is assumed for wave form modeling. The large amplitudes observed for the investigated phases even at large distances from the source suggest that the *P*-to-*S* mode conversion could be favored by the sharp transition at depth from a high-velocity to a low-velocity medium. So a high-velocity

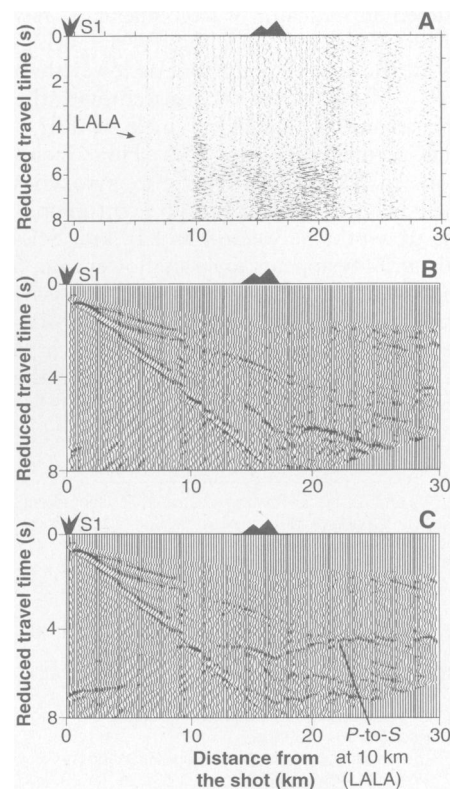


**Fig. 3.** Finite differences modeling of LALA phases. **(A)** Observed horizontal records: the N310°E component, which is oriented along the profile direction. Traces have been bandpass filtered between 1 and 8 Hz. The continuous gray line indicates the approximate arrival of the LALA phase. Reduced travel time is reported on the vertical axis (reduced travel time =  $x/6$ , where  $x$  = distance and 6 km/s is the average velocity of *P* waves in the upper crust). A symbol indicates the location of Mount Vesuvius along the profile. **(B)** Finite differences synthetics computed assuming an increase of *P*-wave velocity at the flat 10-km discontinuity (6.0 to 6.8 km/s). **(C)** Finite differences synthetics computed assuming a sharp decrease of *P*-wave velocity at the 10-km discontinuity (6.0 to 2.7 km/s). The *P*-to-*S* phase is strongly enhanced at about 5 s for distances from the shot larger than 10 to 12 km.

Downloaded from www.sciencemag.org on June 9, 2009

and a low-velocity region below the deep discontinuity were checked in FD wave form modeling. Processed data and FD synthetics obtained assuming a sharp increase in *P*-wave (and *S*-wave) velocity (6.0 to 6.8 km/s) and a sharp velocity decrease (6.0 to 2.7 km/s) at the 10-km discontinuity (Fig. 3) indicate that a velocity decrease as strong as that assumed is needed to generate large-amplitude *P*-to-*S* converted phases. Synthetics produced by this model reproduce the amplitude ratios of *PS* phases and other secondary energetic arrivals that interfere with them in the analyzed distance and time windows.

The occurrence of such mid-crustal high- to low-velocity discontinuities at depths of 10 to 20 km has been observed in several volcanic areas (19), where it is considered an indicator of large magmatic reservoirs. From our modeling, *P*-wave velocity in the low-velocity zone is lower than 2.5 to 3 km/s, which is consistent with the occurrence of magmatic melt within a high-permeability host rock. Fluid inclusions in Mount Vesuvius clinopyroxenes have been trapped at pressure corresponding to depths between 4 and 10 km. Seismic activity appears to be shallower than 6 to 8 km, indicating that the brittle-ductile transition zone is deeper. These data suggest that a melting zone can exist at a depth of 9 to 11 km, as inferred from the analysis of LALA phase.

## REFERENCES AND NOTES

1. V. Arnò *et al.*, in *Somma-Vesuvius*, R. Santacroce, Ed. (Quaderni de La Ricerca Scientifica, Rome, 1987), pp. 53–103.
2. F. Barberi *et al.*, *Bull. Volcanol.* **44**, 295 (1981); L. Civetta, R. Galati, R. Santacroce, *ibid.* **53**, 517 (1991).
3. H. E. Belkin and B. De Vivo, *J. Volcanol. Geotherm. Res.* **58**, 89 (1993).
4. H. Sigurdsson, S. Carey, W. Cornell, T. Pescatore, *Natl. Geogr. Res.* **1**, 332 (1985).
5. P. Papale and F. Dobran, *J. Volcanol. Geotherm. Res.* **58**, 101 (1993).
6. P. Gasparini, M. S. M. Mantovani, R. Scandone, *Bull. Volcanol.* **44**, 317 (1981).
7. R. Santacroce, A. Bertagnini, L. Civetta, P. Landi, A. Sbrana, *J. Petrol.* **34**, 383 (1993); H. E. Belkin, C. J. Kilburn, B. De Vivo, *J. Volcanol. Geotherm. Res.* **58**, 273 (1993).
8. I. Finetti and C. Morelli, *Boll. Geofis. Teor. Appl.* **16**, 175 (1974).
9. C. Principe, M. Rosi, R. Santacroce, A. Sbrana, in *Somma-Vesuvius*, R. Santacroce, Ed. (Quaderni de La Ricerca Scientifica, Rome, 1987), pp. 11–52.
10. E. Cassano and P. La Torre, *ibid.*, pp. 175–196.
11. F. Ferrucci *et al.*, *Geophys. Res. Lett.* **16**, 1317 (1989).
12. The seismic stations (60 of the 82 were three-component digital recorders) deployed along the profile were spaced 250 m apart in the center of the profile (as far as 5 km northwest and southeast of the crater) and 500 m apart at the outer parts. Shot S1 was located on the carbonates of the Sorrento Peninsula, shot S2 was on the southeast slope of the volcano near the Trecase well, and shot S3 was on the south edge of the Mount Somma caldera rim.
13. Mount Vesuvius is presently affected by regular mi-

croseismicity (local magnitude  $M_L < 3$ ) shallower than 5 to 6 km and concentrated beneath Gran Cono, as monitored by the permanent seismic network of Osservatorio Vesuviano. The data from shots S2 and S3 were integrated with arrival times from a selected set of 40 well-located microearthquakes, which provide additional constraints on the deeper part of the volcano edifice. The local earthquakes were preliminarily located in a structure that approximated the 2D initial model used for the tomographic inversion.

14. Methods for travel-time inversion and delay-time tomography were applied to direct *P*-wave arrival times read on the seismic records of shots S2 and S3 at the stations located along the volcano slope. We estimated preliminary 1D velocity profiles for the shallow part of the volcano by using a revised version of the tau-*p* inversion method (20, 21). The 2D shallow structure of Somma-Vesuvius has been determined with a tomographic method in which the propagating medium is described by continuous functions interpolating linearly the velocities assigned to nonregular grid points (21). The ray paths were approximated by an arc of circles, and the solution was obtained by iterative, damped least squares. Space resolution was inferred from ad hoc tests using synthetic data from spike anomalies centered at different positions within the investigated section (21). Resolution is the highest (1.0 km laterally and 0.5 km vertically) at the center of the profile down to a depth of about 4 km and deteriorates laterally and downward.
15. J. Virieux, V. Farra, R. Madariaga, *J. Geophys. Res.* **93**, 6585 (1988); J. Virieux, *ibid.* **96**, 579 (1991).
16. A. Bernasconi, P. Bruni, L. Gorla, C. Principe, A. Sbrana, *Rend. Soc. Geol. Ital.* **4**, 237 (1981).
17. The arrival times of the LALA phase have been modeled by a trial and error approach with the use of a ray-tracing method for a laterally heterogeneous medium (22). A *P*-wave velocity model obtained by tomography was used in the layer above the V-L interface. A linear increase of *P*-wave velocity with depth

with a gradient of 0.05 s<sup>-1</sup> was assumed below the V-L interface. The  $V_p/V_s$  ratio has been assumed to be homogeneous (1.73) for the whole investigated structure.

18. J. Virieux, *Geophysics* **51**, 889 (1986). The equations of motion for elastic velocities and stresses were approximated by FD formulas based on a staggered-grid scheme for space and time steps. Earth's surface was approximated by a discontinuous topography above which stress was assumed to be zero. In our FD simulations, a discretized 2D medium with a grid of points equally spaced in the *x* and *z* directions ( $\Delta x = \Delta z = 50$  m) was used. At each grid point, *P*- and *S*-wave velocity were assigned according to the velocity model used for ray-tracing analysis except that an average velocity profile was used to simulate the velocity variation in shallow volcanic sediments.
19. A. R. Sanford, O. Altepkin, T. R. Toppozada, *Bull. Seismol. Soc. Am.* **63**, 2021 (1973); M. Mizoue, I. Nakamura, T. Yokota, *Bull. Earthquake Res. Inst.* **57**, 653 (1982); S. Matsumoto and A. Hasegawa, *J. Geophys. Res.* **101**, 3067 (1996).
20. E. N. Bessonova, V. M. Fishman, V. Z. Ryaboyl, G. A. Sitnikova, *Geophys. J. R. Astron. Soc.* **36**, 377 (1974).
21. C. H. Thurber, *J. Geophys. Res.* **88**, 8226 (1983).
22. R. De Matteis, A. Zollo, J. Virieux, in preparation; A. Zollo, *et al.*, *Ann. Geofis.*, in press; H. Le Meur, A. Zollo, G. De Natale, J. Virieux, in preparation.
23. We acknowledge two anonymous reviewers for their helpful and critical comments on the manuscript. The seismic tomography of Vesuvius is supported by the Gruppo Nazionale di Vulcanologia, CNR, Italy. This research was cosponsored by the Istituto Italiano di Studi Filosofici, Naples, Conferenza Permanente dei Rettori (Progetto Galileo), and the French embassy in Italy. It was also financially supported through the Ministero per l'Università e la Ricerca Scientifica e Tecnologica (40%) (P.G.).

24 April 1996; accepted 23 July 1996

## Presynaptic Calcium Current Modulation by a Metabotropic Glutamate Receptor

Tomoyuki Takahashi,\* Ian D. Forsythe, Tetsuhiro Tsujimoto, Margaret Barnes-Davies, Kayoko Onodera

Metabotropic glutamate receptors (mGluRs) regulate transmitter release at mammalian central synapses. However, because of the difficulty of recording from mammalian presynaptic terminals, the mechanism underlying mGluR-mediated presynaptic inhibition is not known. Here, simultaneous recordings from a giant presynaptic terminal, the calyx of Held, and its postsynaptic target in the medial nucleus of the trapezoid body were obtained in rat brainstem slices. Agonists of mGluRs suppressed a high voltage-activated P/Q-type calcium conductance in the presynaptic terminal, thereby inhibiting transmitter release at this glutamatergic synapse. Because several forms of presynaptic modulation and plasticity are mediated by mGluRs, this identification of a target ion channel is a first step toward elucidation of their molecular mechanism.

Presynaptic inhibition mediated by the mGluR family (1) has been implicated in autoreceptor inhibition at mammalian glu-

tamatergic synapses (2) and in lateral inhibition at dendrodendritic synapses (3), and more generally in reducing transmitter depletion (4). Presynaptic mGluRs are also crucially involved in the induction of long-term depression at hippocampal mossy fiber-CA3 synapses (5). Pharmacological studies with type-specific agonists indicate that mGluR subtypes 2 and 3 (3, 5) or subtypes 4, 6, 7, and 8 (2, 6) may mediate presynaptic inhibition. Several potential

T. Takahashi, T. Tsujimoto, K. Onodera, Department of Neurophysiology, Institute for Brain Research, Faculty of Medicine, University of Tokyo, Tokyo 113, Japan.  
I. D. Forsythe and M. Barnes-Davies, Ion Channel Group, Department of Cell Physiology and Pharmacology, University of Leicester, Post Office Box 138, Leicester LE1 9HN, UK.

\*To whom correspondence should be addressed. E-mail: ttakahas-ky@umin.u-tokyo.ac.jp